Investigating the contribution of grown new particles to cloud condensation nuclei with largely varying pre-existing particles - Part 1: Observational data analysis

Xing Wei[1#], Yanjie Shen[1,2#], Xiao-Ying Yu[3*], Yang Gao[1,4], Huiwang Gao[1,4], Ming Chu[1], Yujiao Zhu[5], Xiaohong Yao[1,4,6*]

[1]Key Laboratory of Marine Environment and Ecology (MoE) and Frontiers Sci Ctr Deep Ocean Multispheres & Earth, Ocean University of China, Qingdao, China

[2]College of Biology and Oceanography, Weifang University, Weifang, China

[3]Materials Science and Technology Division, Oak Ridge National Laboratory, Oak Ridge, TN 37831-6136, USA

[4]Laboratory for Marine Ecology and Environmental Sciences, Qingdao National Laboratory for Marine Science and Technology, Qingdao, China

[5]Environment Research Institute, Shandong University, Qingdao 266237, China

[6]Sanya Oceanographic Institution (Ocean University of China), Yazhou Bay Science & Technology City, Sanya, China

#Equally contributed to the study; **Correspondence to*: Xiao-Ying Yu (yuxiaoying@ornl.gov) and Xiaohong Yao (xhyao@ouc.edu.cn)

Supplementary text legends:

S1 Operational Details of experiments

S2 Calculation methods

Figure legends:

Fig. S1 The contour plots of particle number size distribution, and times series of N_{ccn}, $N_{cn>100}$, and κ values at 0.2 % and 0.4 % SS on 12–14 July.

Fig. S2 No-NPF days. (2 July (a), 4 July (b), 5 July (c), 7 July (d), 8 July (e), 9 July (f), 10 July (g), 11 July (h)).

Fig. S3 Time series of κ values at 1.0 % on 29 June, 3 July and 6 July.

Fig. S4 ToF-SIMS spectral comparison of atmospheric nanometer particles collected on 30 June (a) and 1 July 2019 (b) in the positive ion mode (m/z^+ 0–200).

Fig. S5 ToF-SIMS spectral comparison of atmospheric nanometer particles collected on 30 June (a) and 1 July 2019 (b) in the negative ion mode (m/z^- 0–200).

Fig. S6 ToF-SIMS spectral comparison of atmospheric nanometer particles collected on 30 June (a) and 1 July 2019 (b) in the negative ion mode (m/z^- 200–350).

Fig. S7 ToF-SIMS selected peak spectral PCA results of 60, 100, and 200 nm particles on 30 June (gray markers) as well as 30 nm, 60 nm, 100 nm, and 200 nm particles on 1 July (red markers) in the negative mode: Scores plots of PC1 vs. PC2 (a), PC1 loadings plots in m/z^- 30–550 (b), and PC2 loading plots in m/z^- 30–550 (c). Peaks are labelled in their center masses.

Table legend:

Table S1. Number concentrations of CN and CCN on NPF days or non-NPF days

Supplementary text

S1 Operational Details of experiments

S1.1 Gas chromatography mass spectroscopy

Measure organic tracers using a gas chromatography mass spectroscopy with an Agilent 6890 GC/5975 MSD. The analyzing procedure was adapted from Kleindienst et al. (2007) and Feng et al. (2013). Briefly, 20mL dichloromethane/methanol (1:1, v/v) was used to extract ultrasonically 25 cm^2 of each quartz filter three times at room temperature, and the extracts combined. The extracts were filtered, dried and then derivatized with 100 μL N,O-bis-(trimethylsilyl)-trifluoroacetamide (BSTFA, containing 1 % trimethylchlorosilane as a catalyst) and 20 μL pyridine at 75 ℃ for 45 min. Surrogate mixture of methylb-D-xylanopyranoside (MXP) and cis-ketopinic acid (KPA) were spiked into the samples as internal/recovery standards before the extraction. Before the injection, hexamethylbenzene was added as an internal standard to check the recovery of the surrogates.

S1.2 Ion chromatography

The operation details of ion chromatography mainly refer to Hu et al. (2005) and Teng et al. (2017). The ion chromatography (Dionex 3000) was used to analyze he inorganic ions in TSP samples. The samples were ultrasonically extracted in deionized water (18 MΩ•cm) at 0 ℃ for 20min. The extracts were filtered through a prebaked Whatman GF/F glass filber filter and then injected to the ion chromatograph equipping with different analytical columns for ion analysis.

S2 Calculation methods

S2.1 Apparent new particle formation rate (FR)

$$FR=\frac{dN_{[d_k,d_u)}}{dt}+\sum_{d_g-d_k}^{d_{u-1}}\sum_{d_i-d_{min}}^{+\infty}\beta_{(i,g)}N_{[d_i,d_{i+1})}-\frac{1}{2}\sum_{d_g=d_{min}}^{d_{u-1}}\sum_{d_i^3=max(d_{min,}^3 d_k^3-d_{min}^3)}^{d_{i+1}^3+d_g^3\leq d_u^3}\beta_{(i,g)}N_{[d_i,d_{i+1})}N_{[d_g,d_{g+1})}+n_u\cdot GR_u \quad (S1)$$

Where FR is the particle formation rate at size d_k, $cm^3\ s^{-1}$, (7 nm in this study); d_u is the upper size limit of the targeted aerosol population (10 nm in this study); d_{min} is the smallest particle size detected by particle size spectrometers (to make the results comparable, the dmin was set to 7 nm); $N_{[dk,du)}$ is the number concentration of particles from size d_k to d_u; d_i represents the lower limit of the i th size bin; $\beta_{(i,g)}$ is the coagulation coefficient for the collision of two particles with the size of di and dg; and GR_u refers to the particle growth rate at size du, nm h^{-1}

S2.2 Net maximum increase in the nucleation-mode particle number concentration (NMINP)

$$NMINP=N_{<30\ nm}(t_1)-N_{<30\ nm}(t_0) \quad (S2)$$

Where $N_{<30\ nm}$ is the sum of nucleation mode particle number concentrations, and t0 and t1 represent the time of an NPF event to be initially observed and the time when $N_{<30\ nm}$ reaches the maximum value, respectively. NMINP equals to N_{dp} in eqution (S1).

S2.3 Multi-lognormal distribution functions

$$f\left(D_p,D_{pg,i},C_i,\sigma_{g,i}\right)=\sum_{i=1}^{n}\frac{C_i}{(2\pi)^{1/2}\log_{(\sigma_{g,i})}}\times\exp[-\frac{[\log\left(D_p\right)-\log(D_{pg,i})]^2}{2\log^2(\sigma_{g,i})}] \quad (S3)$$

Where D_p is the diameter of aerosol particle. Three parameters characterize an individual lognormal mode i: the mode number concentration C_i, geometric variance $\sigma_{g,i}^2$,and geometric mean diameter $D_{pg,i}$.The number of individual lognormal modes that characterize the particle number size distribution is denoted by n(i is in the range of 1–n).In this study, n is usually equal to 2, and $D_{pg,i}$represents the geometric median diameter of new particles followed by particle growth in the observed events. The growth of pre-existing Aitken mode particles was also observed in this study, and $D_{pg,2}$ represents the geometric median diameter of the pre-existing particles.

Figures

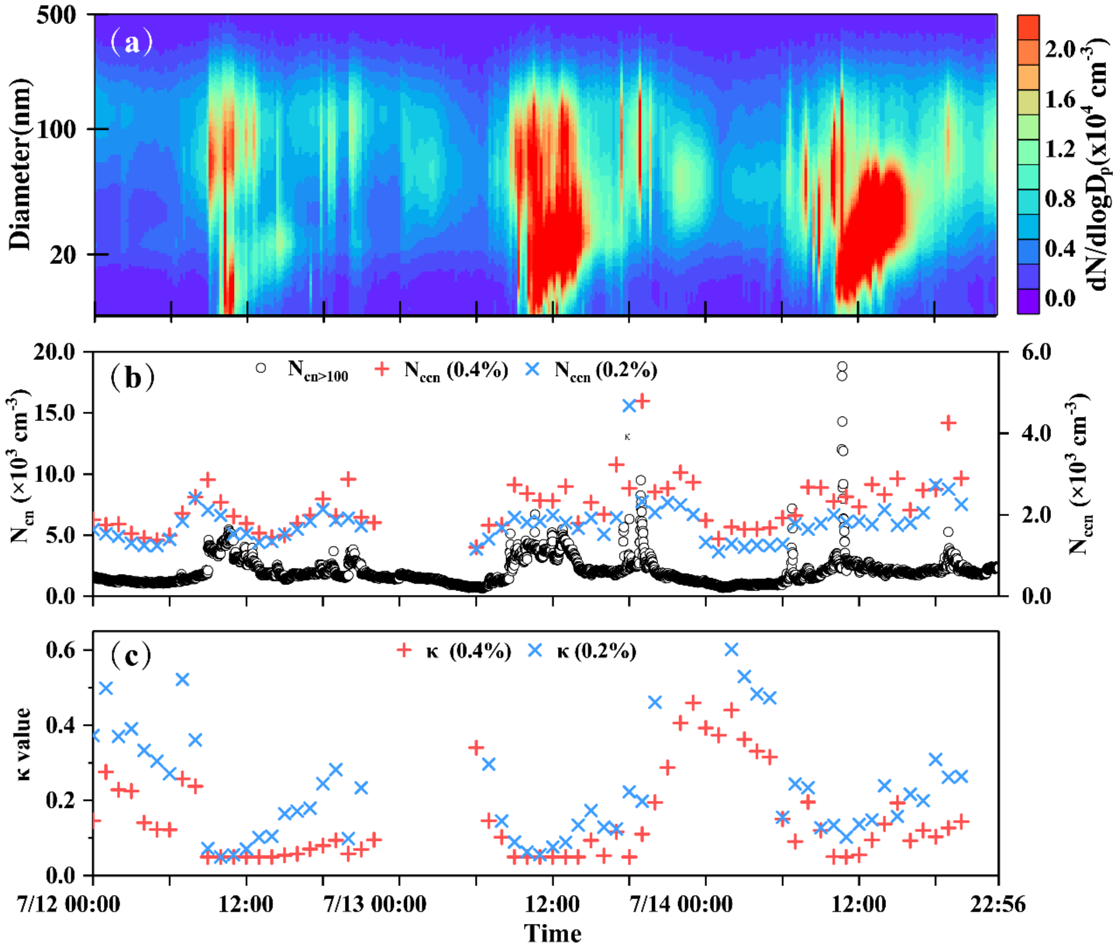

Fig. S1 The contour plots of particle number size distribution, and times series of N_{ccn}, $N_{cn>100}$, and κ values at 0.2 % and 0.4 % SS on 12–14 July.

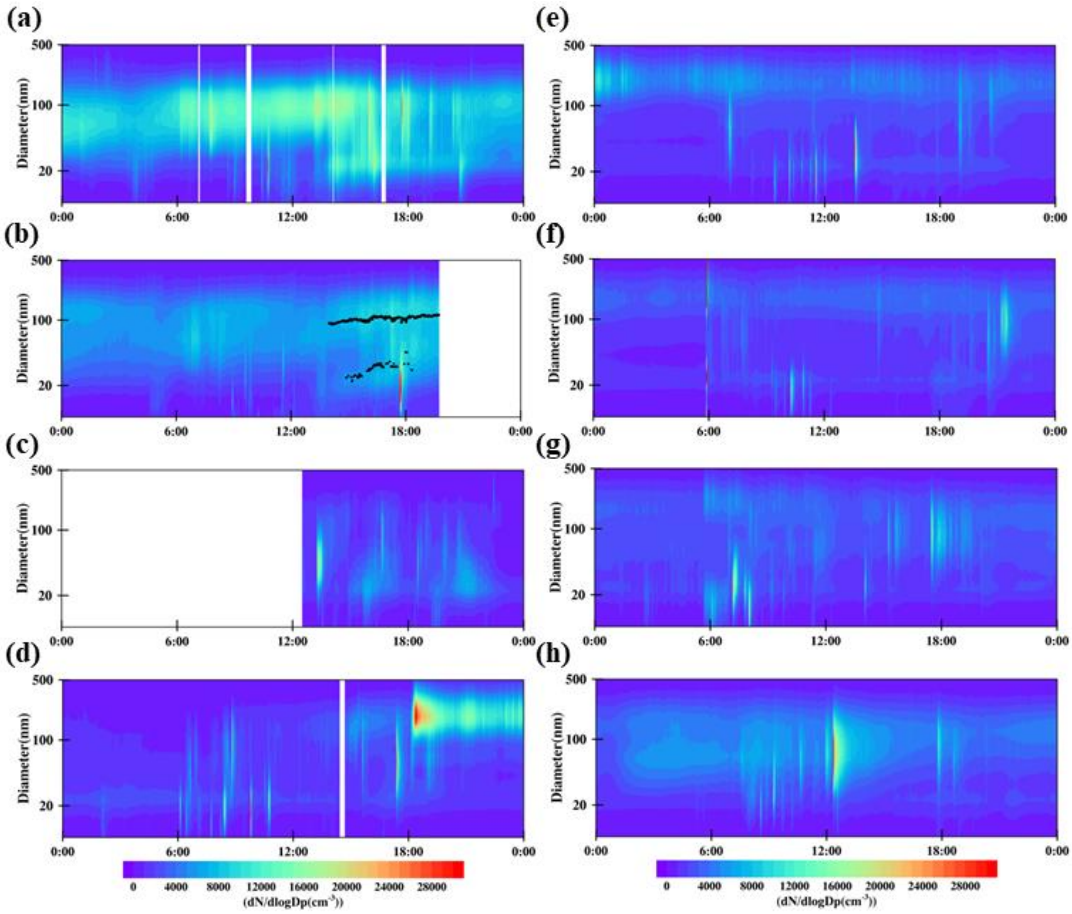

Fig. S2 No-NPF days. (2 July (a), 4 July (b), 5 July (c), 7 July (d), 8 July (e), 9 July (f), 10 July (g), 11 July (h)).

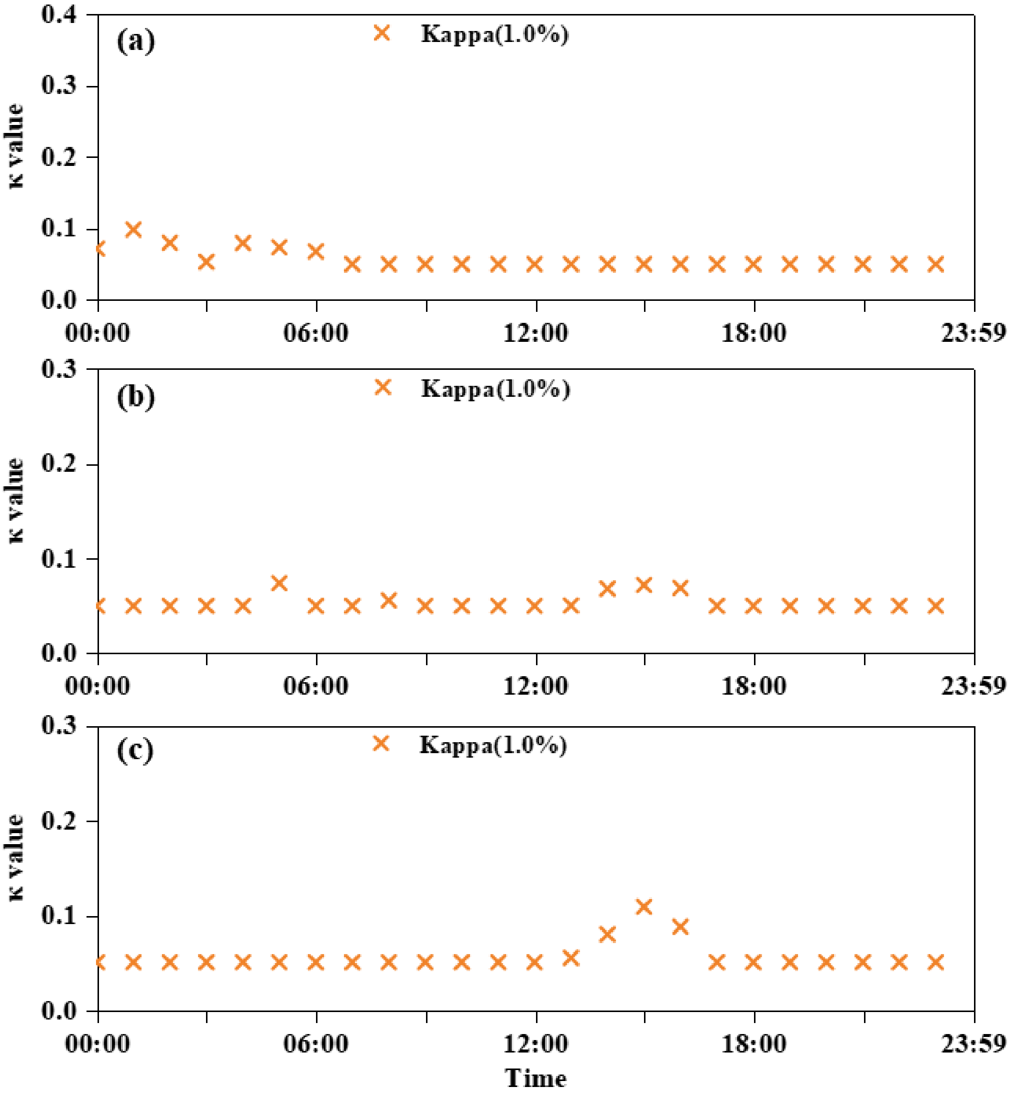

Fig. S3 Time series of κ values at 1.0 % on 29 June, 3 July and 6 July.

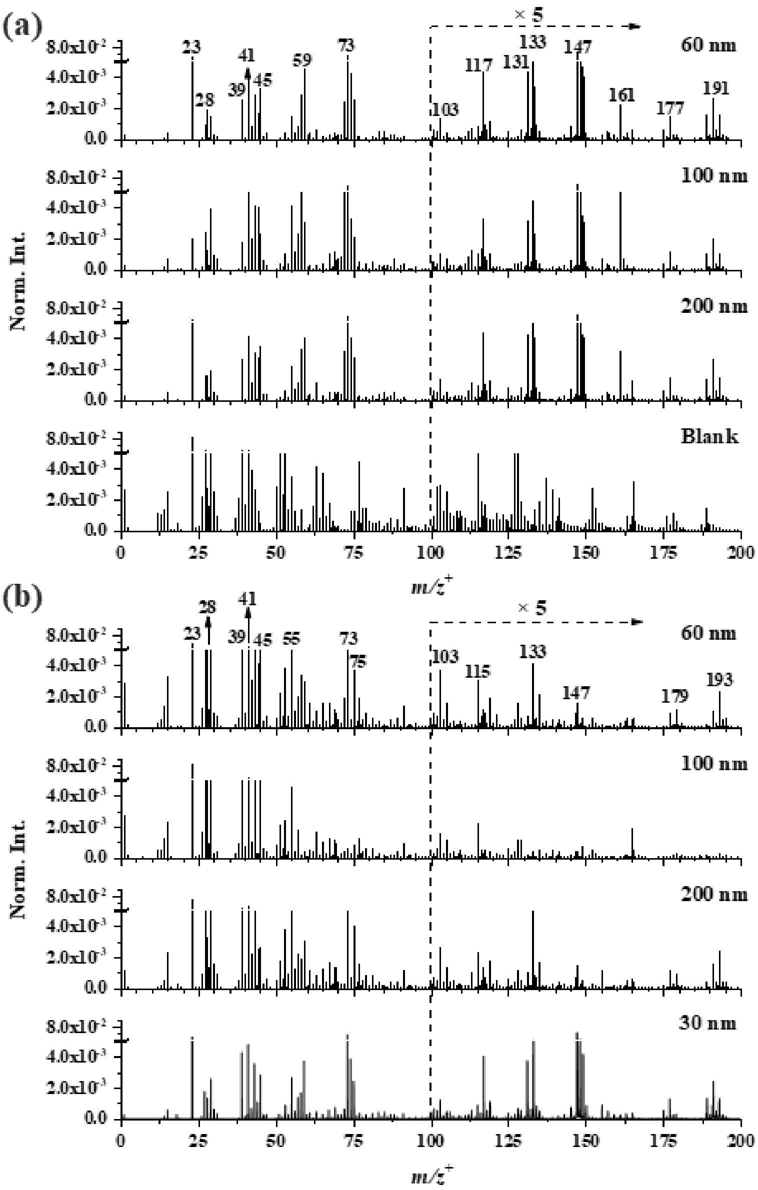

Fig. S4 ToF-SIMS spectral comparison of atmospheric nanometer particles collected on 30 June (a) and 1 July 2019 (b) in the positive ion mode (m/z^+ 0–200).

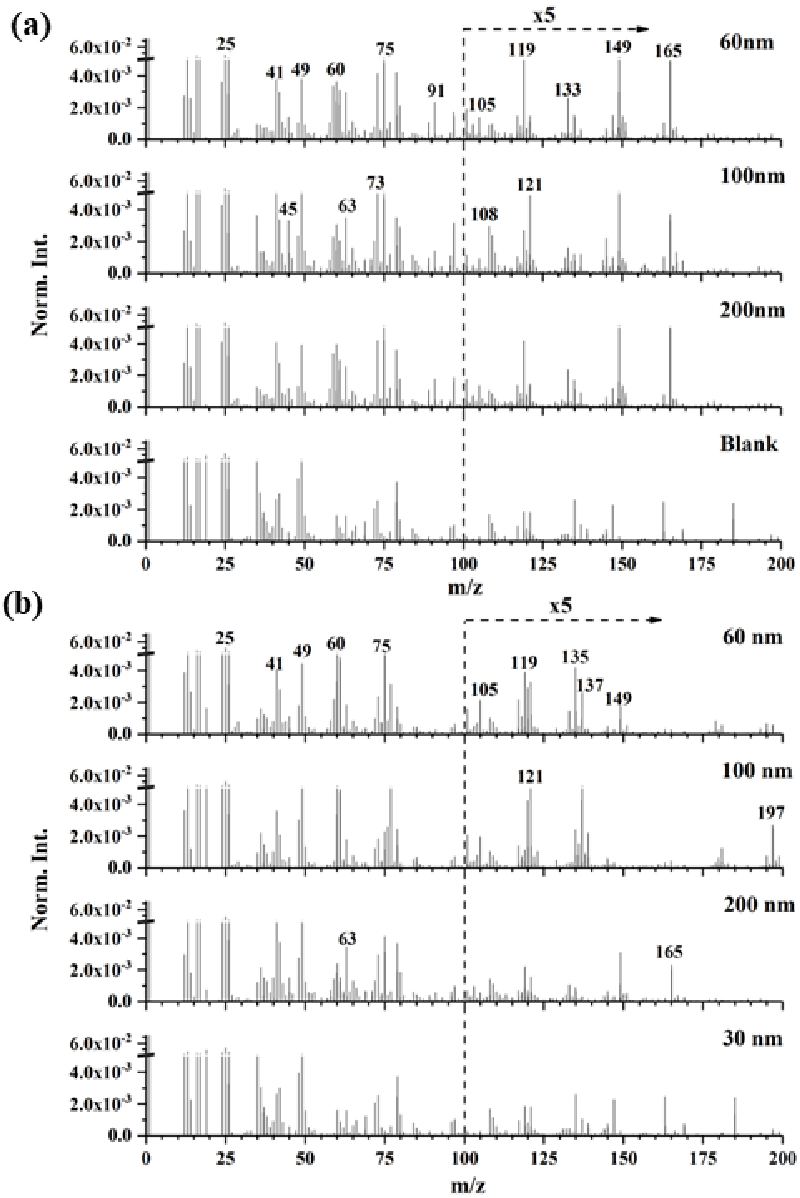

Fig. S5 ToF-SIMS spectral comparison of atmospheric nanometer particles collected on 30 June (a) and 1 July 2019 (b) in the negative ion mode (*m/z*⁺ 0–200).

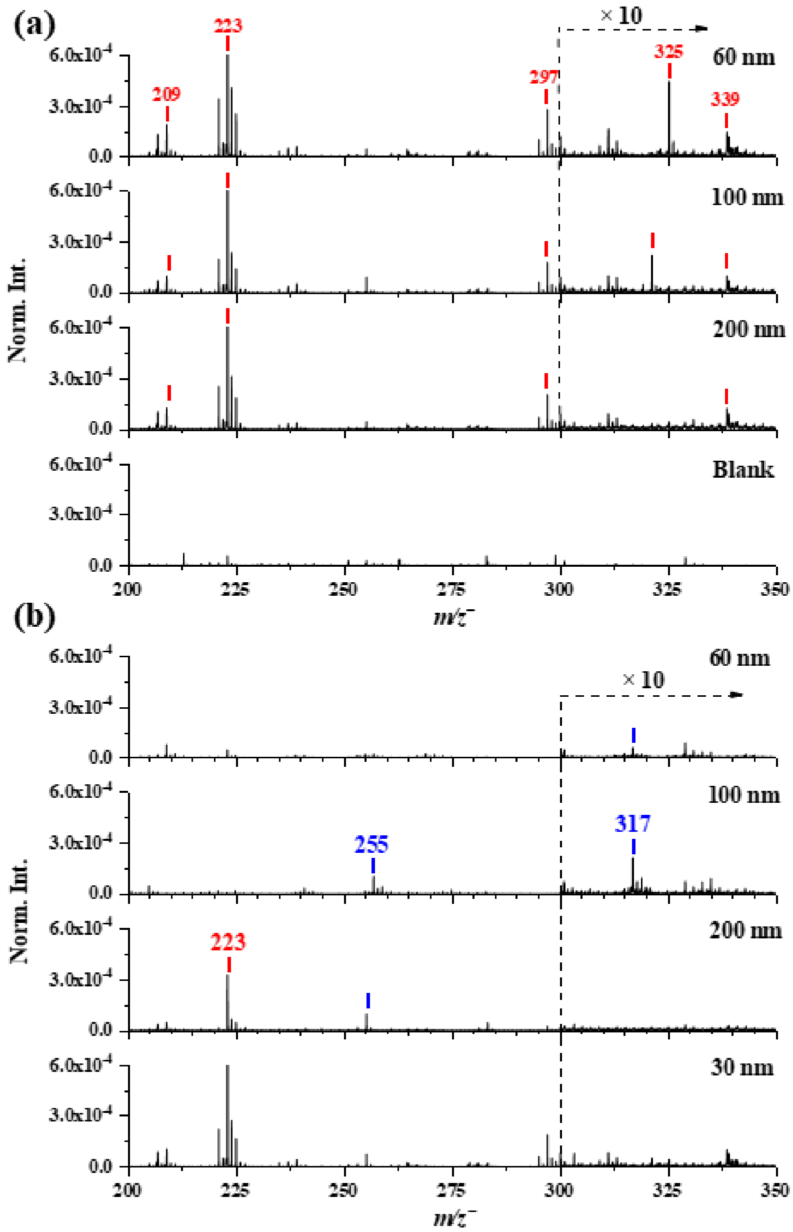

Fig. S6 ToF-SIMS spectral comparison of atmospheric nanometer particles collected on 30 June (a) and 1 July 2019 (b) in the negative ion mode (*m/z*⁻ 200–350).

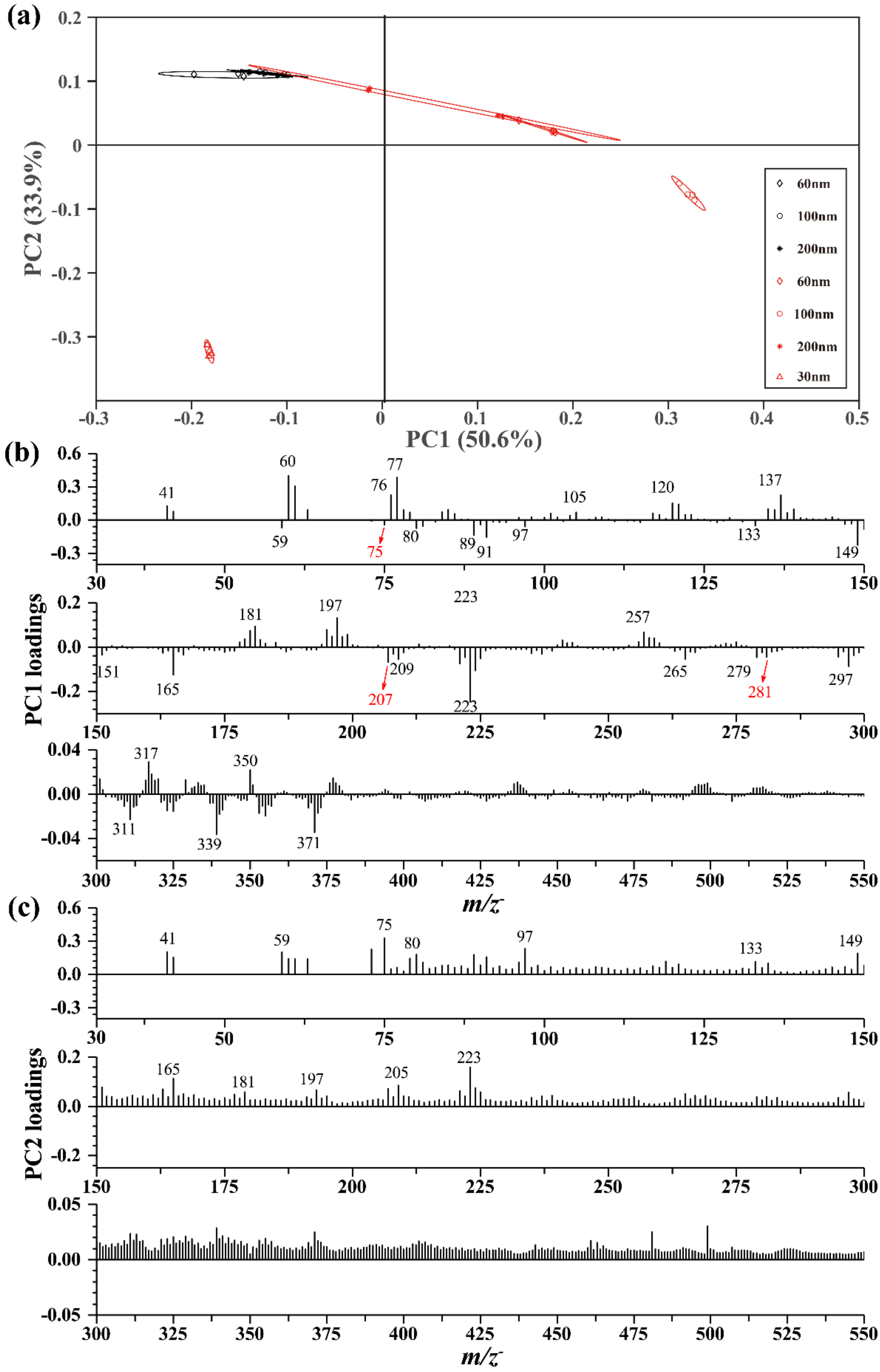

Fig. S7 ToF-SIMS selected peak spectral PCA results of 60, 100, and 200 nm particles on 30 June (gray markers) as well as 30 nm, 60 nm, 100 nm, and 200 nm particles on 1 July (red markers) in the negative mode: Scores plots of PC1 vs. PC2 (a), PC1 loadings plots in *m/z*⁻ 30–550 (b), and PC2 loading plots in *m/z*⁻ 30–550 (c). Peaks are labelled in their center masses.

Table

Table S1. Number concentrations of CN and CCN on NPF days or non-NPF days

	Date	N_{ccn} at five SS levels					$N_{cn>100}$	Total N_{cn}
		0.2 %	0.4 %	0.6 %	0.8 %	1.0 %		
NPF days	29 June	0.7±0.3[a,b]	0.9±0.4	1.0±0.5	1.2±0.6	1.3±0.6	1.3±0.4	7.5±4.3
	30 June	0.6±0.2	0.7±0.2	0.9±0.3	1.0±0.4	1.1±0.6	1.4±0.6	7.4±4.5
	July 1	1.0±0.5	1.4±0.8	1.7±1.0	1.9±1.1	2.1±1.3	1.3±0.3	8.2±5.3
	July 3	1.6±0.5	2.0±0.7	2.3±0.8	2.5±0.8	2.8±0.8	2.0±0.6	9.4±3.2
	July 6	0.6±0.3	0.7±0.4	0.9±0.6	1.0±0.7	1.1±0.8	0.8±0.3	7.5±7.8
	July 12	1.6±0.5	1.8±0.6	1.9±0.8	2.0±0.8	2.2±1.0	2.0±0.9	6.5±4.5
	July 13	1.5±1.2	1.8±1.4	2.1±1.6	2.3±1.7	2.5±1.8	2.1±1.1	10.0±7.6
	July 14	1.7±0.5	2.3±0.8	2.8±0.8	3.1±1.2	3.3±1.2	1.9±1.1	11.0±8.2
	Avg	1.2±0.7	1.5±0.9	1.7±1.1	1.9±1.2	2.1±1.2	1.6±0.8	8.4±6.1
Non-NPF days	July 2	2.4±0.6	2.9±0.6	3.2±0.7	3.4±0.7	3.6±0.8	1.8±0.5	6.1±1.6
	July 4	2.3±0.4	2.7±0.4	3.0±0.4	3.2±0.5	3.3±0.5	2.0±0.5	6.2±1.8
	July 5	1.1±0.9	1.4±1.0	1.6±1.0	1.7±1.1	1.8±1.1	0.6±0.3	3.0±1.4
	July 7	0.8±0.5	0.9±0.5	1.0±0.4	1.1±0.6	1.2±0.6	1.8±2.1	3.6±2.4
	July 8	1.2±0.3	1.5±1.0	1.5±0.7	1.5±0.5	1.6±0.5	1.7±0.4	3.3±1.2
	July 9	1.1±0.7	1.2±0.5	1.4±0.7	1.6±1.2	1.7±1.8	1.4±0.8	3.2±1.8
	July 10	1.5±0.6	1.6±0.6	1.8±0.6	2.0±0.8	2.1±1.0	1.7±0.7	4.5±2.1
	July 11	1.9±0.3	2.2±0.4	2.4±0.5	2.6±0.6	2.8±0.9	1.8±0.4	4.8±1.4
	Avg	1.6±0.8	1.8±0.9	2.0±1.0	2.1±1.1	2.3±1.1	1.7±1.0	4.4±2.1

a. Unit in $\times 10^3$ cm^{-3}.

b. average ± standard deviation.